

Figure 3: Data flow for the BOB@WFI system.

ed once p2pp was run on a different computer than the one where dhs runs.

Data saving continues to be a problem as it consumes a large amount of resources because we have not been able to automate it yet. This will change in the future, once the proper data flow for archiving is implemented.

Figure 3 shows the scheme which we are currently using. The data are backed up every morning from the instrument workstations (w2p2ins) to two DLTs (operations that, together with data verification, take many hours and extend into the early afternoon). One of the DLTs is sent to Garching, while the other is kept at La Silla. Once the tape is "ingested" by the archive in Garching it is returned to La Silla for its reuse (together with the copy that was kept at La Silla). The backup for the Visiting Astronomer is made on DAT tapes from the w2p2off machine. It must be requested daily as there is no room for backlogs. Only raw data are backed up for the Visiting Astronomers.

The backing up of reduced data is their responsibility.

The team is working on an automatic scheme to save data on the w2p2dhs and the w2p2off machines simultaneously to the taking of the data. The main routine has been written and is in the process of debugging. Once they have been fully tested out we will need to assess their impact on the observing efficiency.

3. The future

Among the immediate tasks of the 2p2 Team is the improvement of the Sequencer scripts by making them more efficient and versatile. To this end we are engaged in an effort to parallelise some of the observing tasks, so that the overhead per observation could be reduced. Recent experiments show that without guiding and without filter change, the best we can achieve is 55 s overhead per observation (as opposed to 68 s with the current system). This *fast* mode has resulted in

over 340 frames per night for a programme with a constant integration time of 30 s and no guiding. Such data rates put extreme stress on the operation, and more efficient data archiving methods are urgently needed.

We have also recently experimented with a survey modality of observation, which allows the Visiting Astronomers to align their offsets along lines of constant declination and right ascension for an equinox of their choice, and to specify offsets of any size in their templates. This modality, together with the proper rotation of the instrument will allow for the very precise repetition of previous observations of a large field. We expect to offer these improvements for P68.

One of the main motivations and driving forces behind the development of the VLT-style OS for the WFI is the decision of bringing the WFI to full service mode for period 68. As of this writing (beginning of Period 67), 20% of the assigned time is for service-mode observations. During this time the Team is gaining practice in the use of observing tools such as BOB, P2PP, and OT, to carry out the observations, and it is still getting some of the bugs out of the system.

As mentioned above, among the challenges that we face is the proper data archiving. ESO's Data Management Division is planning to install during July this year the first prototypes of their Next Generation Archive System Technologies, NGA, units at the 2.2-m telescope. This prototype uses swapable SCSI-IDE magnetic disk technology based on a Linux PC system.

The next period with full service mode will be quite challenging, and if it is to succeed it will need the close collaboration between the team in charge of the WFI, the other support teams at La Silla, and the Data Management Division of ESO at Garching. These have certainly been challenging and interesting times and we are motivated by the support of the user community, and of everybody involved.

Achieving 1% Photometric Accuracy with the ESO Wide Field Imager

J. MANFROID (Univ. Liège), F. SELMAN (ESO Chile), H. JONES (ESO Chile)

Introduction

Characterising the accuracy and the precision of photometric observations is notoriously difficult. Although photon statistics, readout noise and other basic parameters offer useful insight into the lower limit of the achievable precision,

actual observations suffer from many additional problems: vagaries of the atmosphere, mismatch between instrumental and standard systems, uncertainties in the standard system, non-linearity of the detectors, and the like. Each source of error has special characteristics with different consequences

for the observations, as is summarised in Table 1.

The highly successful Wide Field Imager (WFI) on the ESO/MPG 2.2-m telescope offers the possibility of undertaking photometry over a half-degree field. Here we discuss findings concerning the photometric perform-

Table 1: Comparison of common sources of photometric errors dependent on colour, intensity, space, time.

Error source	dependent on				possibility for correction	affects		
	colour	intensity	space	time		CM diag.	C index	diff. phot.
Flat field	(x)	–	x	(x)	x	x	(x)	x
Turbulence	(x)	–	–	x	–	(x)	(x)	(x)
Transparency	(x)	–	(x)	x	–	x	x	(x)
Non linearity	(x)	x	(x)	–	x	x	x	x
System mismatch	x	–	–	–	(x)	x	x	–
Photon statistics	–	x	–	–	–	x	x	x

ance of the camera. In particular, we describe strategies for dealing with the flat-field calibration error, which is often underestimated by observers.

Calibration Errors

A recent study by Manfroid et al. (2001) of four telescopes at both ESO and Haute-Provence shows that the amplitude of the flat-field error over the camera area can be of the order of 0.05 mag. Hence, the calibration error must be considered as one of the major sources of uncertainty in CCD photometry.

A component of the flat-field calibration error can be a non-uniform illumination (e.g., a non-uniform twilight sky). However, usually the major contribution comes from scattered light and ghost reflections inside the instrument. Much of this light originates from within the field of view, and even the most careful baffling cannot eliminate the effect.

The insidiousness of the effect is due to the fact that it is a redistribution of light that affects both the science and the flat-field exposures in the same manner. Thus, after dividing the science exposure by the flat-field, one ends up with an image with a very flat sky level, which is what most observers are looking for. However, because the illumination at the mosaic plane was not constant, the result should actually be an image which shows an uneven illumination. Therefore, in this case, a flat sky is a sign of a bad flat field.

The Photometric Super-Flat

We present below two methods for the correction of the data. The first method has been thoroughly tested and has the advantage that one can use the same science observations, if there are enough of them with the proper dithering pattern, to find the correction; the second one, still under development at La Silla, was designed as a quick way to get the *zero-point correction map* (or *photometric super-flat*) with very simple special purpose observations.

Those procedures do not require standard stars and they work with any filter. Obviously, a third, direct, method

can be used if suitable standards can be found all over the camera field. The analysis of a single frame yields the zero-point map. Such standard fields are being set up for the major photometric bands of the WFI.

Method 1. The calibration error can be evaluated – and corrected – by comparing the photometry of stars on dithered exposures (see Manfroid 1995, 1996; Andersen et al. 1995). This procedure yields a purely photometric calibration which has exactly the same purpose as the usual night-sky super-flat: namely, addressing the large-scale trends. Instead of relying on pure background data in median-filtered, blank-sky night frames, the photometric super-flat only uses stellar photometric data and is clearly more suitable.

Suppose we have a number of stars ($s = 1, \dots, S$) recorded on a series of dithered frames ($f = 1, \dots, F$), obtained with various amounts of translation and/or rotation. We assume the frames have been corrected with some high-S/N flat-field calibration (dome or sky), so that high-frequency variations have been removed.

Let $\Psi_{\text{star}}(x)$ be the actual correction needed for stars, and m_s their actual magnitudes. The instrumental magnitudes are $m_{0,f,s}(x)$ and $x = (x, y)$ is the position on the CCD.

We write

$$m_{0,f,s}(x) = m_s + a_f + \Psi(x; b)$$

The parameters a_f are zero-point frame corrections.

$\Psi(x; b)$ is considered to be dependent on a series of parameters $b = \{b_i\}$. It can be developed as a finite series of independent functions $\psi_i(x)$ such as polynomials, but more complex functions can be used. This choice may be crucial. When substantial rotations of the camera are considered, (e.g., alt-az telescopes) the instrumental settings are changed and an angular dependency may have to be introduced.

The parameters a , b and m can be determined by minimising a chi-square function

$$\chi^2 = \sum_{f,s} \sigma_{f,s}^{-2} |m_{0,f,s}(x) - m_s - a_f - \sum_i b_i \psi_i(x)|^2$$

where $\sigma_{f,s}$ is the precision on the magnitude measurement (f, s).

Under even limited photometric conditions (a_f constant for at least three frames), simple dithered sequences suffice to yield a robust solution. Otherwise it is necessary to know the precise photometry of at least three stars. Combining rotations and translations is an alternative, not always feasible, and which introduces instrumental changes.

In order to get the best accuracy, one can combine all available photometric data from dithered frames observed during an observing run. The observations must have been obtained under similar instrumental conditions and processed with the same flat field calibration. This means that tens or hundreds of frames can be used in each band.

Method 2. This second method, just a variation of the previous one, was developed by one of the authors (Selman 2001), because it was important for the La Silla team in charge of the 2.2-m telescope to have a procedure that could be carried out as part of the standard calibration plan. The requirements for such a procedure are that it should use as little telescope time as possible, and that the data analysis should be straightforward. As mentioned above, it is possible to do a quick calibration with the use of only three dithered exposures per filter. We have developed a method that, if used with three exposures of an adequately dense stellar field, taken in quick succession, permits an adequate calibration (residual errors $\approx 1\%$). The three exposures should be a central exposure, a second exposure with a right ascension offset, and a third exposure with a declination offset. One should cross identify stars in the frames and perform aperture photometry on them. The photometry is then corrected for any overall zero point shifts that could be caused by transient atmospheric transparency fluctuations between exposures. Then, the mosaic is divided in sub-areas numbered 1 to N. The areas are chosen such that their sizes correspond to the amplitude of the offsets. Thus, each star has its magnitude measured in at least two areas, with an observed magnitude difference dm_{obs} .

If we knew the difference in zero points between the different sub-areas,

we could calculate the magnitude differences measured above. Even if we do not know the zero point differences, we can calculate them with the following procedure: assign to sub-area i , a zero point z_i , and estimate for each dm_{obs} , a corresponding dm_{calc} . In matrix notation, if each row of a *design* matrix represents a single magnitude difference, and the columns represent the different sub-areas, we can write $dm_{\text{calc}} = A \cdot z$, where z is a vector with the zero points for each sub-area, and A is the design matrix, with as many columns as the number of areas in which the mosaic has been subdivided, and as many rows as stellar magnitude differences that have been measured. This matrix is made of mostly zeros, and has the values of 1 and -1 at the two positions corresponding to the areas where the magnitude difference is being computed. One can then determine the values of z which minimise $\|dm_{\text{obs}} - dm_{\text{calc}}\|^2$. The solution to this least-square problem is given by the *normal equations*

$$(A^T \cdot A) \cdot z = A^T \cdot dm_{\text{obs}}$$

This linear system is ill-defined unless we design the observations properly. That is why we need offsets in both directions. We also need to fix the value of the zero-point in one of the mosaic sub-areas. For the details on how to solve these equations, see Selman (2001).

Results with the WFI

Figure 1 shows contour plots of *UBVR I* flat-field corrections obtained over a two-night observing run with the ESO WFI, using the first method described in the previous section. Figure 2 shows perpendicular profiles through the CCD. The results presented here correspond to a particular set of dome flat fields. The screen was illuminated with a lamp except for the *U* flats which were obtained with day light.

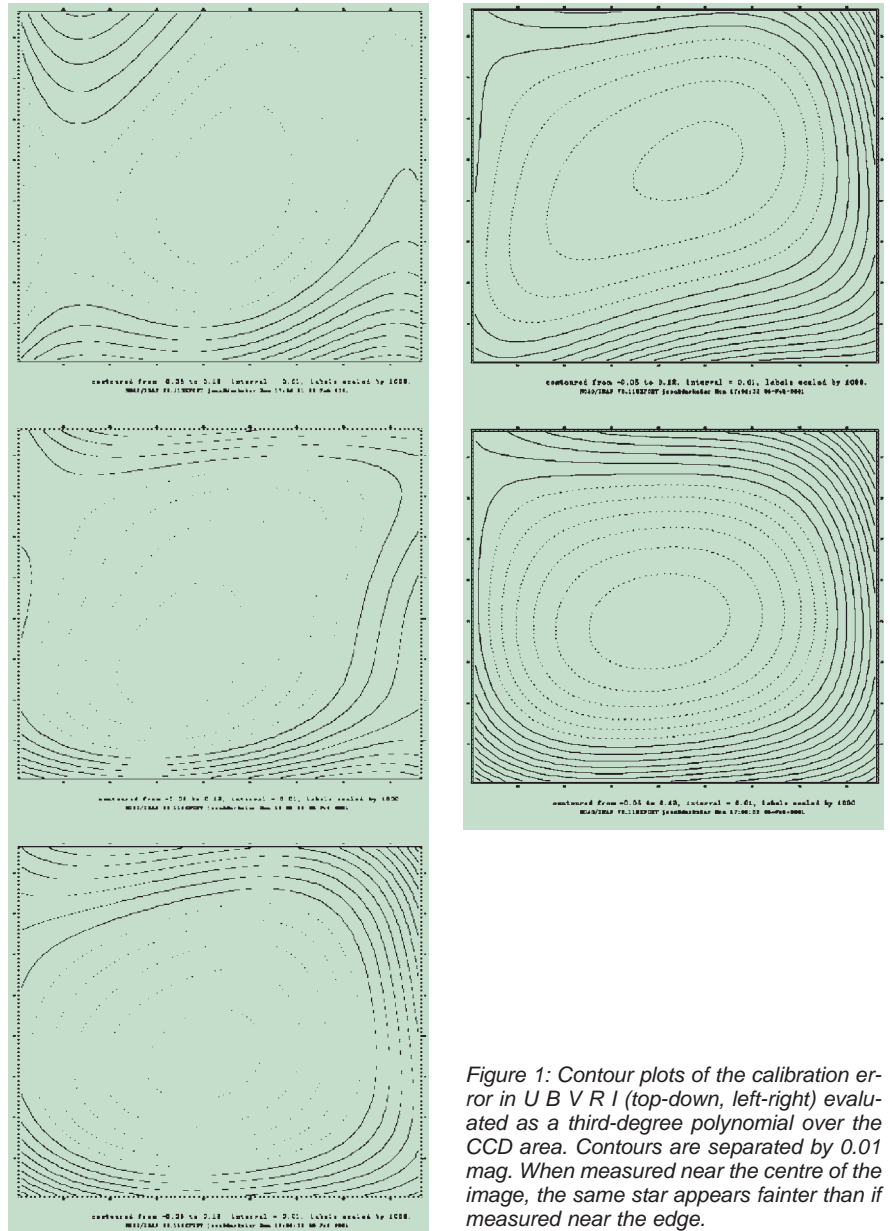


Figure 1: Contour plots of the calibration error in *UBVR I* (top-down, left-right) evaluated as a third-degree polynomial over the CCD area. Contours are separated by 0.01 mag. When measured near the centre of the image, the same star appears fainter than if measured near the edge.

The illumination conditions were therefore quite different and this explains the peculiar characteristics of the *U* calibration correction. The correction that

must be applied to the regular dome, twilight, or super sky-flats, always results in a relative dimming of their central areas with respect to the areas

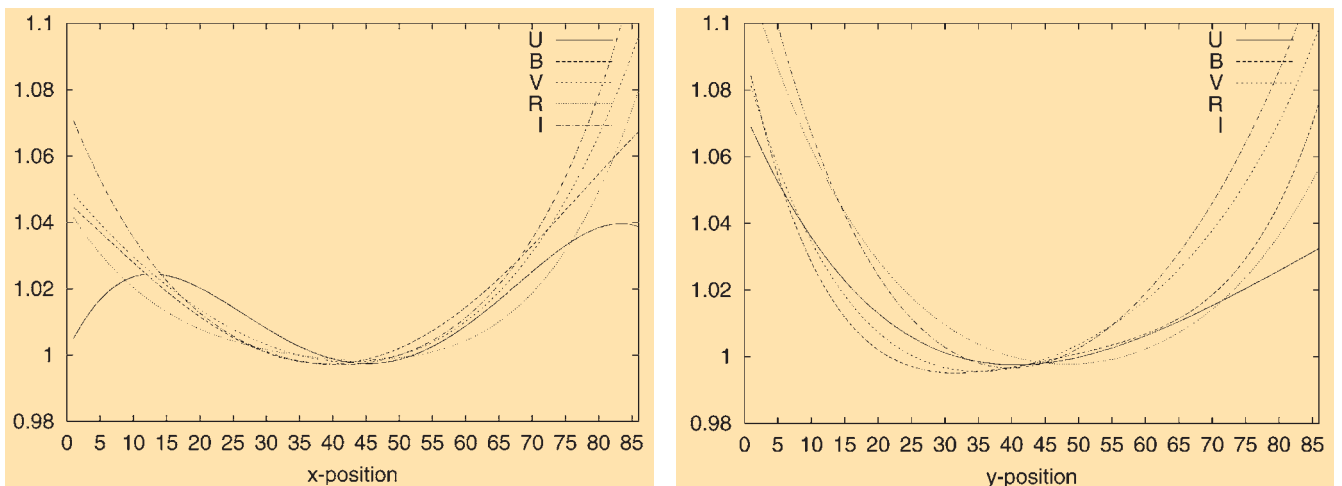


Figure 2: Central cross section of the calibration correction in RA (left) and dec (right). The correction is normalised to unity in the central area.

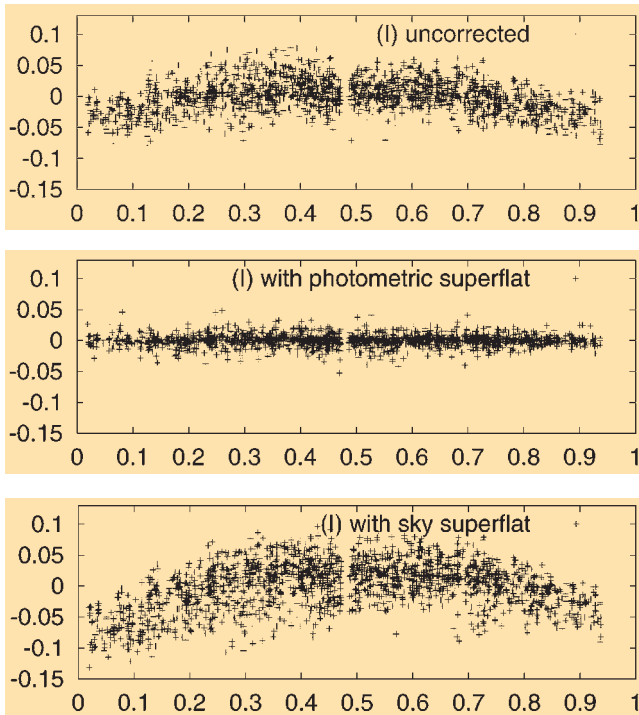


Figure 3: Observed deviations to the average I magnitude as a function of position (declination in relative units) for 400 stars observed on 34 exposures in 7 distinct fields. The upper plot shows data processed through the usual flat-field technique. In the middle plot the correction (“photometric super-flat”) has been applied. The lower plot shows the same results when a night-sky super-flat calibration is used instead.

away from the centre. This will result in a brightening of the sky background in the central areas of the science images, together with a brightening of the stars in the same areas (see Figs. 2 and 3).

Figure 4 shows the results of applying the second method to a totally independent data set. The points depict the local V magnitude differences with an offset of only 30 arcsecs. The solid line is a solution zero point curve, that is, it is the magnitude that has to be added to each stellar magnitude as a function of position on the mosaic. This solution corresponds to a one dimensional analysis of a strip 1000 pixels wide, along the declination direction of the mosaic. A cursory look to the data shows that the agreement with the results from method 1 is roughly at the 1% level.

The correction tends to be larger at longer wavelengths. Scattering and/or reflections by the optical elements may be less important at shorter wavelengths. Another explanation is that the contrast between the screen and the surrounding surface of the dome may be higher in the blue and UV, hence the relative amount of scattered light decreases.

It is logical to expect that sky flats contain a larger proportion of scattered light than dome flats obtained with a correctly-sized screen. Indeed, this is what has been observed at various telescopes (Manfroid et al. 2001), including the WFI. Images processed with

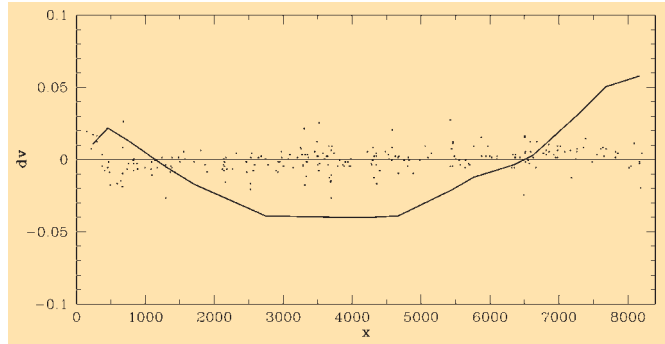


Figure 4: The points show the differences in magnitude between measurements performed on the same stars, but separated by 30 arcseconds in RA. The solid curve shows the zero point difference as a function of position in the mosaic, obtained with the second method described in the text. It is noteworthy that the stars used to make the graph are extremely bright, with DAOPHOT estimated errors much smaller than 1 mmag; nevertheless, the scatter in the magnitudes is only slightly less than 10 mmag.

twilight or night sky flats need larger corrections. This is illustrated in the lower panel of Figure 3 which shows that the worst photometric results are obtained with a night-sky super-flat – a technique that is often claimed to offer the best calibration.

However, when using dome flats with the WFI, it is advisable to check each new set against an old one, since variations in the illumination pattern have been noted on rare occasions (Jones et al. 2000). We have also found for the WFI that although dome flats taken with a lamp do not do a good job at removing features such as *dust donuts*, dome flats with Sun light do.

Stray Light Contribution

All optical systems exhibit the effects of stray light at some level. Usually it is

seen in the form of spurious reflections (“ghost images”) originating between different combinations of optical surfaces. It is commonly a problem in imaging instruments such as focal reducers, that carry several air-glass surfaces. It is not uncommon to see families of ghost reflections following distinct exponential or diametric patterns, depending on the geometry of the optics (see e.g. Jones, Shopbell & Bland-Hawthorn 2001). Such internal reflections can be largely minimised (< 1%) through suitable anti-reflection coatings, typically consisting of a quarterwave layer of MgF_2 , or multi-layer coatings of alternating MgF_2 and TiO_2 . Alternatively, silica sol-gel coatings have recently been demonstrated to give superior performance over traditional coatings (Stilburn 2001), and they are now being used in place of MgF_2 for some astronomical instruments with many air-glass surfaces.

The ESO WFI consists of two lens triplets and the filter is located between them in a converging $f/5.9$ beam. There are nine air-glass surfaces, including

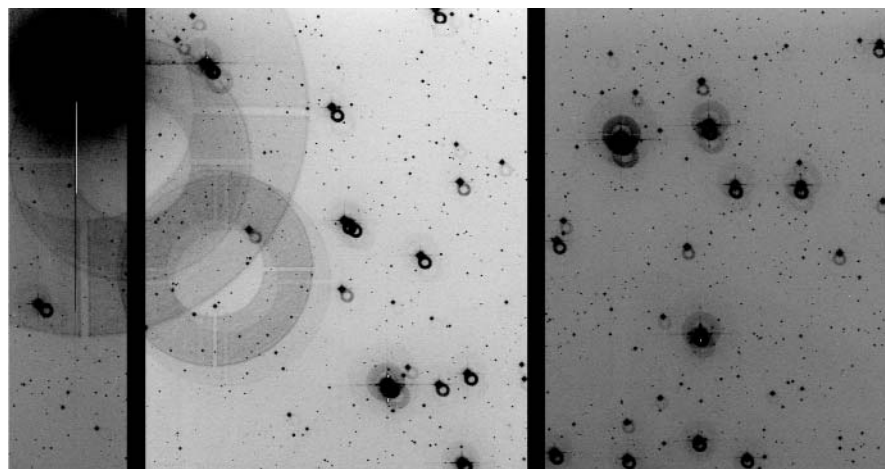


Figure 5: Ghost reflections seen in the $H\alpha$ filter on a portion of the WFI mosaic. Most stars show a primary reflection (smallest and nearest to the star). Secondary and tertiary reflections are also visible on a few of the brighter stars while the very bright star in the top left shows ghost images almost as large as an entire CCD, due to multiple internal reflections, many times over.

the CCD dewar entrance window and the surface of the CCD itself. The most obvious spurious reflections in WFI images are out-of-focus ghost images of bright stars (Fig. 5). The effect is at least partly filter-dependent – multiple reflections are much more prevalent in the H α and [S II] narrow-band filters compared to other narrow-bands or *UBVR I*. Individual ghost reflections in *BVR I* contain 1.5 to 2% of the unreflected starlight; the reflections in H α and [S II] are even stronger than the others because the first reflection is nearer to focus, and the light more concentrated, even though the total reflected content is virtually the same. Removing these ghosts from sky frames is somewhat problematic, since the offset between ghost and object varies symmetrically with object distance from the optical axis. Hence, telescope dithering and median-filtering strategies such as those described in Jones, Shopbell & Bland-Hawthorn (2001) are not effective.

Ghost reflections are just one contributor to stray illumination in the flat-field. Other components such as diffuse scattered light (across the full field), focal concentration and side illumination also contribute, giving rise to flat-field errors discussed earlier. These are not as readily identifiable as the ghosts, and so at best, the observer needs to correct for their influence through the offset technique described above. The bottom line is that the combined contribution is more than a few per cent, and observers desirous of

photometric precision better than a few per cent need to correct for these effects.

Conclusions

Considering the field size of the WFI camera, the flat-field errors are not unusually large. This bears testimony to the quality of the optics. However, for many observers, the amplitude of the effect might come as a surprise since it is often claimed in the literature that cameras in general can be flat-fielded to within a few millimagnitudes (particularly when using median filtered night-sky frames as super-flat calibration). A perfect calibration should *not* leave a flat sky background if the illumination at the detector plane is not uniform, hence this should not be considered as a valid test of the achieved accuracy. We have shown that if we use just the standard flat-field correction, the achievable accuracy is of the order of 5%. Nevertheless, this number does not contain the whole truth because the same star placed at different parts of the mosaic could show systematic variations in its measured brightness of almost 10% peak-to-valley. This is quite devastating for programmes that attempt to find spatial correlations in quantities directly derivable from the fluxes. Thankfully, the colours appear to be much less affected.

One may wonder why such errors are rarely accounted for. It is simply not easy to detect the 2-D effect unless you specifically look for it, and have suitable

dithered frames to analyse. It is reassuring to see that with the proper procedures the systematic errors can be reduced down to 1%.

Because of a fast readout and the large area – hence, the large number of measurements per frame – WFI observations can easily include the dithered exposures needed for computing the calibration correction. This procedure will still be easier when accurate wide-field standard fields are available.

References

- Andersen M.I., Freyhammer L., Storm J., 1995, in “Calibrating and understanding HST and ESO instruments”, Ed. P. Benvenuti, ESO Conference and Workshop Proceeding No. **53**, 87.
- Jones, D. H., Shopbell, P. L., Bland-Hawthorn, J., 2001, *MNRAS*, submitted (http://www.sc.eso.org/hjones/WWWpubl/detect_meas.ps.gz).
- Jones, D.H. and the 2p2 Team, 2000, “Inspection of Flatfields from the Decontamination Monitoring Programme” (<http://www.lis.eso.org/lasilla/Telescopes/2p2T/E2p2M/WFI/documents/Decontam/FFofWFI.ps.gz>).
- Manfroid J., 1995, *A&AS*, **113**, 587.
- Manfroid J., 1996, *A&AS*, **118**, 391.
- Manfroid, J., Royer, P., Rauw, G., Gosset, E. 2001, in *Astronomical Data Analysis Software and Systems X*, ASP Conference Series, in print.
- Selman, F. J., 2001, “Determining a zero-point variation map for the WFI.” (<http://www.lis.eso.org/lasilla/Telescopes/2p2T/E2p2M/WFI/zeropoints>).
- Stilburn, J., 2000, in “Optical and IR Telescope Instrumentation and Detectors” Eds. M. Iye and A. F. M. Moorwood, *Proc SPIE* 4008.

SCISOFT – a Collection of Astronomical Software for ESO Users

R. HOOK, ST-ECF

There are active astronomers, visitors and students at all four ESO sites who need a wide variety of software to work efficiently. Much of this scientific software has been developed in the community and is not normally used in non-astronomical establishments. Examples are software to reduce, display, analyse and visualise astronomical data.

If there is no co-ordination, there is a strong tendency for such software to be installed at the different sites only when requests come from users and there is no simple way, or enough human resources, to make updates or ensure compatibility between sites. As a result it was common for visitors to ESO sites to be unsure what software they could expect to be available and in the case of offline data manipulation at the tele-

scope such uncertainty could lead to inconvenience and possibly inefficient use of observing time.

To try to avoid these problems the Scisoft project was established at the beginning of 2000. It is a joint effort between the author from the ST-ECF, the ESO scientific community represented by an advisory board with delegates from each ESO site, and the ESO IT group which is part of the Technology Division. Recently, the Data Management and Operations Division has also become an active member by supporting external distribution.

Scisoft maintains a uniform, documented and tested collection of software for the three main ESO computer platforms – Solaris, HP-UX and Linux – and makes regular distributions internally on CD-ROM. This collection is the

standard one for users and visitors at all four sites. It is also distributed from Garching to Chile using mirroring so that updates propagate automatically. The items included on the three platforms are close to identical. At each release the policy is to have only one version of each package, the most recent available. Installing a single collection takes far less effort than locating and installing many individual items and testing them and hence leads to a major reduction in the total effort required for scientific software support throughout ESO.

The content of the collection is driven by the needs of ESO users which are expressed by representatives of all four ESO sites at a board meeting before each new release. At present the collection contains IRAF with many lay-

